Spontaneous Formation of Dipolar Metal Nanoclusters†

Sara E. Mason,‡ Elizabeth A. Sokol, Valentino R. Cooper,§ and Andrew M. Rappe*

The Makineni Theoretical Laboratories, Department of Chemistry, University of Pennsylvania, Philadelphia, Pennsylvania 19104-6323

Received: November 30, 2008; Revised Manuscript Received: February 5, 2009

The adsorption of three- and four-atom Ag and Pd clusters on the α-Al_2O_3 (0001) surface is explored with density functional theory. Within each adsorbed cluster, two different cluster−surface interactions are present. We find that clusters simultaneously form both ionic bonds with surface oxygen and intermetallic bonds with surface aluminum. The simultaneous formation of disparate electronic structure motifs within a single metal nanoparticle is termed a "dipolar nanocluster". This coexistence is ascribed to a balance of geometric constraints and metal electronic structure, and its importance for nanoparticle catalysis is highlighted.

There is great fundamental interest in understanding how transition metals and oxides are affected by contact with each other.[1] A prevailing question is how to characterize the electronic interactions at the metal/oxide interface. This interest is driven by the desire to harness the effects of interfacial metallic tuning on catalytic properties.[2−9] Studies in the literature show that both size[4,9−14] and identity[15−19] of the deposited metal cluster play a role in determining the chemistry at the metal/oxide interface. Recent theoretical work by Hinnemann and Carter reveals that the electronic interactions at the interface depend strongly on identity of the deposited metal.[20] Through a systematic study of Al, O, Hf, Y, Pt, and S atoms on the (0001) surface of α-Al_2O_3, they were able to distinguish different bonding motifs. The more electronegative species (O, S, Pt) formed covalent-type bonds. The electropositive atoms (Al, Hf, Y) exhibited an ionic interaction, transferring charge to the surface.

Experimental studies of the deposition of Ag monomers, dimers, and trimers on TiO_2 indicate that differences in deposited cluster mobilities directly influence cluster nucleation sites, size, and geometry.[11] The spatial extent of even small deposited metal particles usually results in nonuniform interfacial interactions, due to the interplay of the geometry of the substrate lattice and metal−metal bonding. In the present work, we report a novel consequence of how clusters accommodate these factors: small supported Me_n clusters (Me = Ag, Pd) exhibit two coexisting structural and electronic relationships to an Al_2O_3 substrate. The close proximity of such different states within one cluster is fundamentally interesting and has ramifications for understanding and improving noble metal nanocluster catalysis. We use first-principles density functional theory (DFT) to study the bonding of three- and four-atom Me clusters to α-Al_2O_3. We find that cluster size and the substrate geometry influence stable adsorption structures, while the identity of the deposited metal influences interfacial electronic structure.

DFT calculations were performed with a generalized-gradient approximation exchange-correlation functional[21] as implemented in an in-house code. All calculations were converged using a 2 × 2 × 1 grid of Monkhorst−Pack *k*-points.[22] Norm-conserving optimized pseudopotentials[23] with the designed nonlocal method for metals[24,25] were constructed using the OPIUM pseudopotential package.[26] The Kohn−Sham orbitals are expanded in a plane-wave basis set truncated at 50 Ry. Cluster adsorption is modeled on one side of the slab, and a dipole correction[27] is used to remove any artificial effects on the structural and electronic properties arising from periodic boundary conditions.

The Al_2O_3 surface is modeled by a slab geometry supercell with an in-plane $(\sqrt{3}\times\sqrt{3})R30°$ unit cell and periodic boundary conditions. The slabs consist of five $Al_3O_9Al_3$ trilayers, making the surfaces Al-terminated. At least 12 Å of vacuum separate periodic images in the (0001) direction. The theoretical Al_2O_3 in-plane lattice constant of 4.85 Å is used. Full relaxation of all layers is allowed (and required) to ensure insulating behavior in the clean slab. Structural details of the optimized surface are consistent with other modeling studies.[28−30]

Three Ag_n clusters were considered for adsorption to the surface: Ag_3, planar Ag_4, and pyramidal Ag_4. To find minimum energy structures, each cluster was placed in three different starting positions on the surface. Interfacial Ag atoms were started at top, bridge, or hollow sites of the oxygen lattice, and each system was allowed to relax fully. Optimization of these nine unique starting structures resulted in two final structures, one for Ag_3 and one for Ag_4. Based upon the two-dimensional character of the optimized Ag_4 cluster on Al_2O_3, and also due to the likelihood that electrostatic interactions with the surface would be screened by base atoms in a three-dimensional cluster,[31] only Pd_3 and planar Pd_4 adsorption geometries were modeled, in starting positions like those described for Ag_n.

The results are discussed by first presenting the structural details of the adsorbed Me_n clusters. The optimized Ag_3/Al_2O_3 structure is shown in Figure 1 (optimized Ag_4/Al_2O_3 structure in Figure 2). The structure can be understood by rationalizing the optimization trajectory from the hollow site initial configuration. The O−O distance (≈2.8 Å) in the topmost $Al_3-O_9-Al_3$ trilayer allows the Ag_3 to begin in three adjacent hollow sites, one site centered above a surface Al, one above a subsurface Al, and the third centered above a second trilayer Al. Upon optimization, the Ag over the surface Al rises away from the surface. The Ag over the subsurface Al moves both in-plane toward a second surface Al and away from the surface.

† Part of the "George C. Schatz Festschrift".

* To whom correspondence should be addressed. E-mail: rappe@sas.upenn.edu.

‡ Current address: National Institute of Standards and Technology, 100 Bureau Drive Stop 8553, Gaithersburg, Maryland 20899.

§ Current address: Materials Science and Technology Division, Oak Ridge National Laboratory, Oak Ridge, TN 37831-6114.

10.1021/jp8105088 CCC: $40.75
Published on Web 03/16/2009

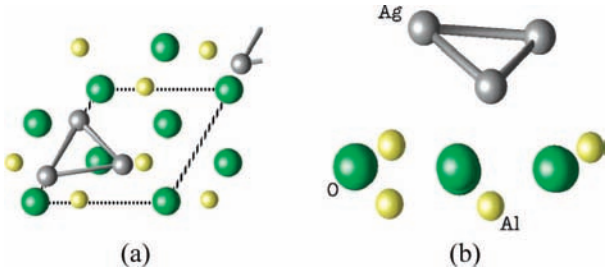

Figure 1. Top (a) and side (b) views of optimized Ag_3/Al_2O_3 structure. The surface cell is shown by dashed lines. Oxygen atoms are green, Ag atoms are gray, and Al are gold. The distance between the two raised Ag atoms is 2.85 Å. The other two Ag−Ag distances are 2.62 Å.

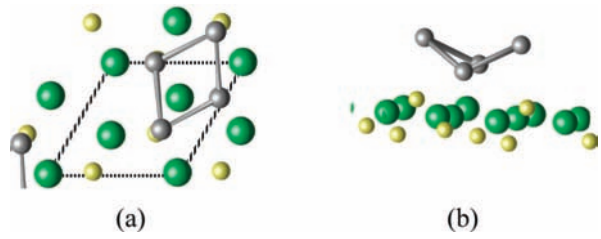

Figure 2. Top (a) and side (b) views of optimized Ag_4/Al_2O_3 structure. The surface cell is shown by dashed lines. Oxygen atoms are green, Ag atoms are gray, and Al are gold. The Ag−Ag distances are all approximately 2.7 Å.

The third Ag remains in the hollow site with no topmost trilayer Al and stays relatively close to the surface. Thus, one Ag atom is bound to the surface oxygen atoms and two Ag atoms make a short bond with an Al atom. The resulting structure has an Ag_3 triangle tilted away from the surface by 33° and shows significant topmost Al relaxation. Defining z as the distance of Al atoms from the topmost oxygen layer in the surface normal direction, bare Al_2O_3 has $z = 0.09$ Å for the topmost Al layer. In response to cluster adsorption, the nearest surface Al atoms move vertically by $\Delta z = -0.45$, $+0.36$, and $+0.42$ Å. Two pairs of Ag and Al shift upward together. The inward relaxation of the other nearby surface Al atom induced by metal cluster adsorption has been observed in other theoretical work.[32]

The relaxed interatomic distances strongly suggest two different bonding motifs. In Ag_3/Al_2O_3, the raised Ag and Al make short bonds of 2.76 Å on average, similar to the sum of their covalent radii ($r_{Ag} = 1.53$ Å, $r_{Al} = 1.18$ Å). The shortest distance from these Ag atoms to O is 3.23 Å on average, longer than the sum of their ionic radii ($r_{Ag^+} = 1.14$ Å, $r_{O^{2-}} = 1.24$ Å). The other Ag atom has a short 2.28 Å distances to O, quite in line with ionic bonding. This Ag atom also has a long distance of 3.05 Å to subsurface Al, suggesting little, if any, covalent interaction in that case. The bond length data can be summarized as an intermetallic (IM) bond between the raised Ag and Al, and ionic Ag−O bonds for the other Ag atom. Similar analysis of the other Me_n/Al_2O_3 structures supports the classifications of IM and ionic cluster/surface bonding.

To visualize the electronic cluster/surface interactions, we study the change in charge density induced by the cluster adsorption:

$$\Delta\rho = \rho_{Ag_n/Al_2O_3} - \rho_{Ag_n} - \rho_{Al_2O_3} \quad (1)$$

where ρ_{Ag_n/Al_2O_3} is the charge density of the adsorbed Ag_n/Al_2O_3, and ρ_{Ag_n} and $\rho_{Al_2O_3}$ are the charge density of the isolated systems fixed to their adsorbed geometries for Ag_n and Al_2O_3, respectively. The side views of the iso-surfaces for $\Delta\rho$ in Ag_n/Al_2O_3 are presented in Figure 3, with electronic charge flowing from dark to light regions. Figure 3 shows gain of charge between raised Ag−Al pairs, indicative of Ag−Al IM bond formation. The other Ag atom shows a significant loss of electrons, with a corresponding gain of electrons for the nearest topmost surface oxygens. Therefore, these interactions are chiefly ionic bonds.

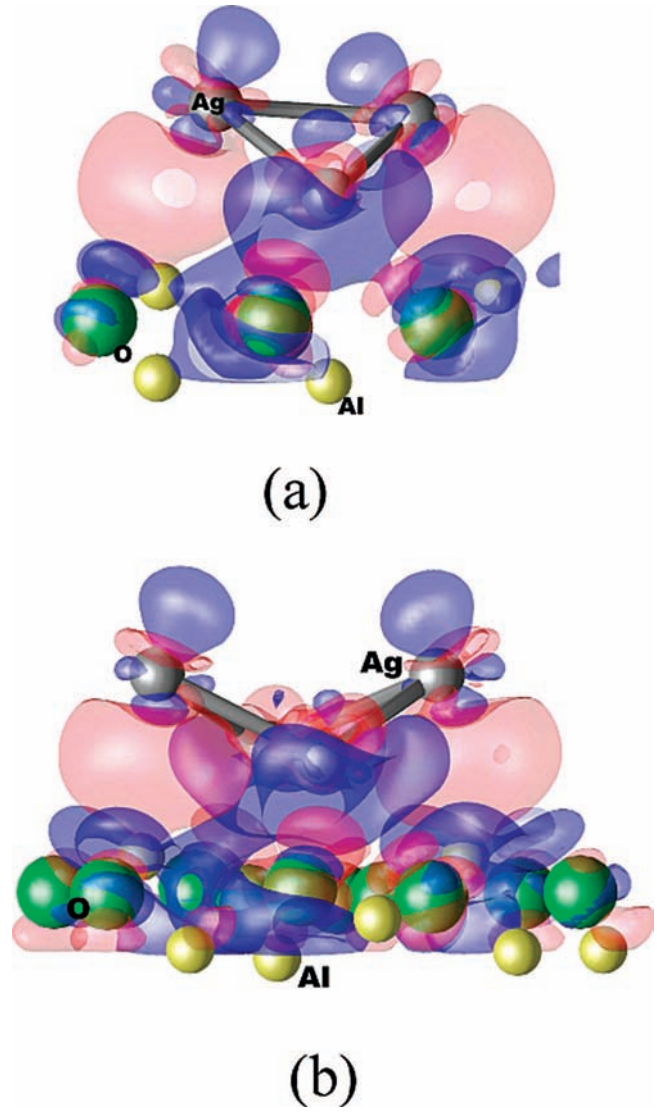

Figure 3. Induced charge density $\Delta\rho$ diagrams for the optimized structure of Ag_n/Al_2O_3. O (green), Ag (black, connected), and Al (gold) are shown as spheres of decreasing size. Adsorption causes electron flow from dark (blue) to light (red) regions. Iso-surface values are ±0.02 $e^-/Å^3$. (a) Ag_3/Al_2O_3, (b) Ag_4/Al_2O_3.

The observed surface relaxations show clear effects of the two different surface−cluster bonding motifs. In Ag_3/Al_2O_3, the ionic bond formed between Ag and O leaves the O atom less capable of bonding to surface Al atoms, using a bond-valence argument.[33] Therefore, the adjacent surface Al atom relaxes inward (below the top O layer) to form bonds with subsurface oxygen. The increase in electron density near the IM Al atoms reduces electrostatic interactions with oxygen and results in the observed outward relaxations.

The electronic description of Me_n adsorption bonding also provides insight into the adsorption energies of the clusters. Comparison of E_{ads} data in Table 1 shows that adsorption of an additional Me atom results in a slight increase in E_{ads} for the Ag and Pd clusters, 0.26 and 0.07 eV, respectively. The

TABLE 1: Adsorption Energies (eV per Cluster) E_{ads} and Shortest Me−O and Me−Al Bond Lengths (Å) for Me_n/Al_2O_3[a]

	E_{ads}	Me_{ionic}−O	Me_{IM}−O	Me_{ionic}−Al	Me_{IM}−Al
Ag_3	1.71	2.28	3.23	3.05	2.76
Ag_4	1.97	2.45	3.50	3.03	2.63
Pd_3	2.51	2.19	2.77	2.91	2.56
Pd_4	2.58	2.26	3.32	2.90	2.50

[a] Bond lengths are average for each atom type (ionic, IM) in each cluster.

TABLE 2: Fractional Filling of the s-Bands (f_s), Average Energy of the d-Band Projections (ε_d), and the Change in System Dipole As the Supported Metal Atoms Are Displaced in the (0001) Direction ($\Delta(\mu)/\Delta(z_{Me})$), for Atoms in Supported Clusters[a]

	f_s	ε_d, eV	$\Delta(\mu)/\Delta(z_{Me})$, *e*
Ag_3 Ionic	0.33	−3.18	0.32
Ag_3 IM	0.56	−3.58	−0.01
Ag_4 ionic	0.33	−3.23	0.26
Ag_4 IM	0.67	−3.63	−0.04
Pd_3 ionic	0.38	−1.50	0.35
Pd_3 IM	0.50	−1.25	0.05
Pd_4 ionic	0.47	−1.59	0.27
Pd_4 IM	0.59	−1.58	0.00

[a] Quantities are averaged for ionic and IM atoms in each cluster.

adsorption energy of the cluster can be thought of as a difference between the energies of the surface−cluster bonds formed upon adsorption and the energies of the internal surface and cluster bonds which are broken or weakened due to the presence of the cluster. In particular, the creation of strong ionic Me−O bonds weakens the bonds between the Me atoms of the cluster. For the Me_3 cluster, the two IM Me atoms are close to each other and can compensate for the weakened bonds between IM and ionic Me atoms. The geometry of the Me_4 cluster, however, means that the two IM Me atoms are separated from each other and can only bond to ionic Me atoms. Thus, for the adsorbed Me_4, the bond energy gained from additional Me−O bonds is counterbalanced by the bond energy lost through the weakening of all five Me−Me bonds in the cluster.

We propose referring to these clusters as "(electric) dipolar nanoparticles." (Magnetic) dipolar nanoparticles have been reported,[34] but we know of no previous report showing spontaneous formation of electric dipoles on nanosized supported metal particles.

Ionic and IM Me/surface interactions are also revealed in atom-projected density of states (PDOS) analysis. Intermetallic bonding causes orbitals to mix, leading to intensity in the IM Me s-PDOS below the Fermi level. The s-orbitals of the ionic Me atoms show less intensity at bonding levels and are dominated by substantial intensity above the Fermi level. The fractional fillings f_s of the Me s-bands are presented in Table 2 for all studied Me_n/Al_2O_3. The distinction between the IM and ionic bonding interactions is well represented in the s-PDOS of Ag_4/Al_2O_3, as shown in Figure 4.

The projection onto Me d-states suggests that the coexistence of two cluster/surface interactions affects the reactivity of the supported Me atoms, as larger chemisorption energies for a wide variety of adsorbates are known to be favored by higher energy d-states and disfavored by the lower energy d-states.[35] Our analysis shows that the filling of the supported Me d-bands is constant, near unity for all Ag atoms and near 0.9 for all Pd atoms. Table 2 lists the average energy of the d-band projections

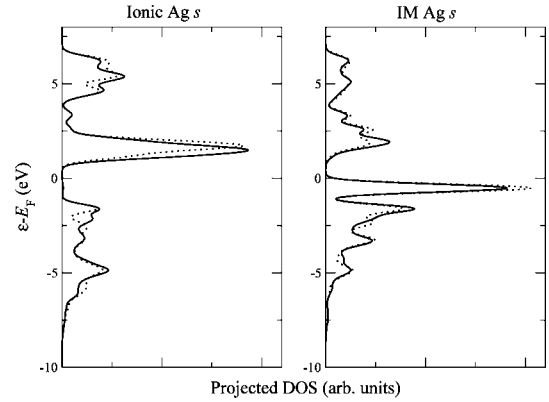

Figure 4. Density of states projected onto the s-orbital of Ag atoms in Ag_4/Al_2O_3. There are two ionic and two IM Ag atoms in the adsorbed cluster, and the projections are done atom by atom. The solid and dashed lines in each plot show the s-projections of both of the ionic Ag atoms (left) and both of the IM Ag atoms (right).

(ε_d) of supported Me atoms with respect to the Fermi level. ε_d is well established as a predictive parameter for assessing reactivity.[35] The 0.40 eV shift in ε_d between the ionic and IM Ag atoms in Ag_n/Al_2O_3 is larger than what can be achieved through perturbations such as strain[36,37] and is more in line with the extent of shift brought about by significant coordination change[38] or introduction of a metal heteroatom to a surface.[39] The shift in ε_d between the ionic and IM Pd atoms in Pd_n/Al_2O_3 is smaller, up to 0.25 eV.

To further investigate the charge state of the supported metal atoms, we use the calculation of Born effective charges. The Born effective charge is defined as the change in the total system dipole as a particular atom is displaced. The advantage of this approach is that such an atomic charge is well-defined. We examine the changes in the system dipole along the (0001) direction and calculate $\Delta(\mu)/\Delta(z_{Me})$. This derivative is calculated using finite difference and atomic displacements of ±0.3 Å in 0.1 Å increments. Values reported in e are given in Table 2. The positive (negative) values of $\Delta(\mu)/\Delta(z_{Me})$ for ionic (IM) supported Me atoms represent positive charge moving from (toward) the cluster as the atom is raised.

On the basis of the structural and electronic results, we can assess how cluster size, surface geometry, and cluster identity differently influence the metal/oxide interactions. The isostructural relationship between the supported Ag_n and Pd_n clusters indicates that cluster size and surface morphology strongly influence the geometry of adsorption. In the case of Me_3 on Al_2O_3, only one Me−Al IM bond can be formed at equilibrium. We observe in-plane cluster distortion and migration that accommodates a second, elongated Me−Al bond. For clarity in discussing and presenting results, we classify this interaction as IM, though it has both IM and ionic character. In the case of Me_4, the cluster's long diagonal length is similar to the inherent Al−Al separation in the (0001) plane. Therefore, two Me−Al interactions can exist while maintaining Me occupation of hollow sites. On the basis of similarities in Me−Me bond lengths across the transition metal series, we expect that other small metal clusters would adsorb similarly on Al_2O_3. However, varying the substrate facet or composition would impose different constraints on adsorbing metal clusters, and would likely lead to different trends in adsorption geometries.

While the identity of the deposited metal is only a minor influence on the adsorption geometry, it clearly governs various aspects of the electronic structure. Our analysis of the PDOS (Table 2) shows that the distinction between IM and ionic Me

f_s and ε_d is greater for supported Ag_n than for Pd_n. This is the result of the greater metallic character of Pd clusters. In the limit of cluster sizes of just a few atoms, the unfilled d-band does not fully bar dipolar character in the cluster. However, the distinction between Pd atoms is precarious, as even small displacements from the optimized Pd_4 positions induce changes in the total DOS at E_F. This suggests that, on a given surface, a nanoscale transition between dipolar and bulklike cluster electronic structure exists, with a metal-dependent cluster critical size.

In conclusion, we find both ionic Me−O and intermetallic Me−Al interactions in metal clusters adsorbed on the alumina surface. The proximal coexistence of these interactions results in the formation of dipolar nanoparticles. The electronic and structural effects are closely related, with IM and ionic Me−surface bonding favoring outward and inward Al motion, respectively. We find consistent results and interpretations of induced charge density, dipole, and PDOS in all optimized cluster geometries. Along with trends and roles of the substrate, cluster size, and choice of metal, the identification of coexisting ionic and IM bonding in supported clusters will enhance the understanding of cluster deposition, nucleation, and growth processes. The reported metal/oxide interactions also have significant implications when applied to the field of catalysis and may lead to the introduction of novel supported nanocatalysts.

Acknowledgment. We acknowledge Ilya Grinberg and Anne M. Chaka for valuable discussions and thank Ilya Grinberg for reviewing the manuscript. This work was supported by the Air Force Office of Scientific Research, Air Force Materiel Command, USAF, under Grant No. FA9550-07-1-0397 and by the Department of Energy Office of Basic Energy Sciences, under grant no. DE-FG02-07ER15920. Computational support was provided by the HPCMO. S.E.M. was supported in part by a National Research Council (NRC) Postdoctoral Fellowship.

References and Notes

(1) Fu, Q.; Wagner, T. *Surf. Sci. Rep.* **2007**, *62*, 431.
(2) Roberts, S.; Gorte, R. J. *J. Chem. Phys.* **1990**, *93*, 5337.
(3) Petrie, W. T.; Vohs, J. M. *J. Chem. Phys.* **1994**, *101*, 8098.
(4) Haruta, M. *Catal. Today* **1997**, *36*, 153.
(5) Walter, E. J.; Lewis, S. P.; Rappe, A. M. *Surf. Sci.* **2001**, *495*, 44.
(6) Bozo, C.; Guilhaume, N.; Herrmann, J.-M. *J. Catal.* **2001**, *203*, 393.
(7) Molina, L. M.; Hammer, B. *Phys. Rev. Lett.* **2003**, *90*, 206102.
(8) Chen, M. S.; Goodman, D. W. *Science* **2004**, *306*, 252.
(9) She, X.; Flytzani-Stephanopoulos, M. *J. Catal.* **2006**, *237*, 79.
(10) Eichler, A. *Phys. Rev. B.* **2003**, *68* (1), 205408.
(11) Benz, L.; Tong, X.; Kemper, P.; Lilach, Y.; Kolmakov, A.; Metiu, H.; Bowers, M. T.; Buratto, S. K. *J. Chem. Phys.* **2005**, *122*, 081102.
(12) Asthagiri, A.; Sholl, D. S. *Phys. Rev. B* **2006**, *73*, 125432.
(13) Finnis, M. W. *J. Phys.: Condens. Matter* **1996**, *8*, 5811.
(14) Valero, M. C.; Raybaud, P.; Sautet, P. *Phys. Rev. B* **2007**, *75*, 045427.
(15) Zhukovskii, Y. F.; Fuks, D.; Kotomin, E. A.; Ellis, D. E. *Nucl. Instrum. Methods Phys. Res. B.* **2007**, *255*, 219.
(16) Krischik, S.; Stracke, P.; Höfft, O.; Kempter, V.; Zhukovskii, Y. F.; Kotomin, E. A. *Surf. Sci.* **2006**, *600*, 3815.
(17) Grau-Crespo, R.; Hernández, N. C.; Sanz, J. F.; de Leeuw, N. H. *J. Phys. Chem. C* **2007**, *111*, 10448.
(18) Carter, E. A.; Goddard, W. A., III *J. Catal.* **1988**, *112*, 80.
(19) Carter, E. A.; Goddard, W. A., III *Surf. Sci.* **1989**, *209*, 243.
(20) Hinnemann, B.; Carter, E. A. *J. Phys. Chem. C* **2007**, *111*, 7105.
(21) Perdew, J. P.; Burke, K.; Ernzerhof, M. *Phys. Rev. Lett.* **1996**, *77*, 3865.
(22) Monkhorst, H. J.; Pack, J. D. *Phys. Rev. B* **1976**, *13*, 5188.
(23) Rappe, A. M.; Rabe, K. M.; Kaxiras, E.; Joannopoulos, J. D. *Phys. Rev. B Rapid Comm.* **1990**, *41*, 1227.
(24) Ramer, N. J.; Rappe, A. M. *Phys. Rev. B* **1999**, *59*, 12471.
(25) Grinberg, I.; Ramer, N. J.; Rappe, A. M. *Phys. Rev. B* **2001**, *63*, 201102(R).
(26) http://opium.sourceforge.net.
(27) Bengtsson, L. *Phys. Rev. B* **1999**, *59*, 12301.
(28) Verdozzi, C.; Jennison, D. R.; Schultz, P. A.; Sears, M. P. *Phys. Rev. Lett.* **1999**, *82*, 799.
(29) Wang, X.-G.; Chaka, A.; Scheffler, M. *Phys. Rev. Lett.* **2000**, *84*, 3650.
(30) Ruberto, C.; Yourdshahyan, Y.; Lundqvist, B. I. *Phys. Rev. B* **2003**, *67*, 195412.
(31) Cooper, V. R.; Kolpak, A. M.; Yourdshahyan, Y.; Rappe, A. M. *Phys. Rev. B* **2005**, *72*, 081409(R).
(32) Gomes, J. R. B.; Lodziana, Z.; Illas, F. *J. Phys. Chem. B* **2003**, *107*, 6411.
(33) Brown, I. D. In *Structure and Bonding in Crystals II*; O'Keeffe, M., Navrotsky, A., Eds.; Academic Press: New York, 1981; pp 1−30.
(34) Ditsch, A.; Laibinis, P. E.; Wang, D. I. C.; Hatton, T. A. *Langmuir* **2005**, *21*, 6006.
(35) Hammer, B.; Morikawa, Y.; Nørskov, J. K. *Phys. Rev. Lett.* **1996**, *76*, 2141.
(36) Mavrikakis, M.; Hammer, B.; Nørskov, J. K. *Phys. Rev. Lett.* **1998**, *81*, 2819.
(37) Mason, S. E.; Grinberg, I.; Rappe, A. M. *J. Phys. Chem. C* **2008**, *112*, 1963.
(38) Hammer, B.; Nielsen, O. H.; Nørskov, J. K. *Catal. Lett.* **1997**, *46*, 31.
(39) Ruban, A.; Hammer, B.; Stoltze, P.; Skriver, H. L.; Nørskov, J. K. *J. Mol. Catal. A: Chem.* **1997**, *115*, 421.

JP8105088